E. Synge: Microscopy with holes

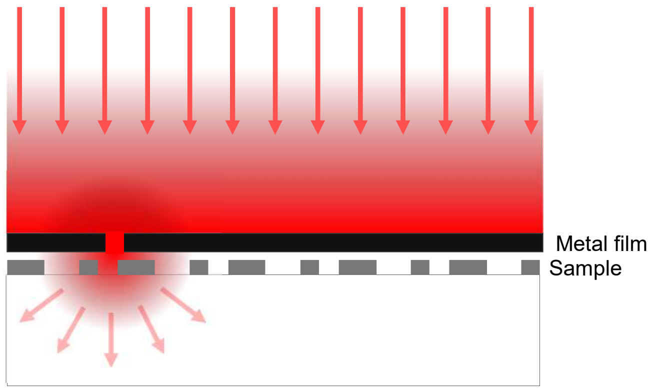

E. Synge (1928)

E. H. Synge (1928)

XXXVIII. *A Suggested Method for extending Microscopic Resolution into the Ultra-Microscopic Region.* By E. H. Synge*.

1890 - 1957

…

It remains to consider the most obvious technical difficulties. These seem to be four in number :—

(1) The source of illumination, which must be of very great intensity.

(2) The making of small adjustments of order 10^{-7} cm., which would be required in the vertical inter-adjustments of the section and the opaque plate, and the making of regular increments of motion of 10^{-6} cm. in the plane of the section, the conditions in both cases being such that friction cannot be entirely eliminated.

(3) The planing of the biological section so that it presents a surface which does not diverge from a plane by more than a fraction of 10^{-6} cm.

(4) The construction, in an opaque plate or film, of a hole whose diameter is of the order 10^{-6} cm.

Scanning Near-Field Optical Microscopy (SNOM): A Brief Historical Overview

1928 E. H. Synge: Microscopic Imaging by scanning a submicroscopic light source across a sample

1956 J. A. O'Keefe: „Resolving Power of Visible Light“

1956 A. V. Baez: Experiments with sound waves

1972 Ash & Nicholls: Micro-wave experiment with sub-wavelength sized apertures at a resolution of $\lambda/60$.

1984 D. Pohl, W. Denk & M. Lanz: Demonstration of a resolution of $\lambda/20$ using visible light.

…

1991 E. Betzig et al.: „Breaking the Diffraction Barrier – Optical Microscopy on a Nanometric Scale“

…

Near-Field Imaging with a Tapered Probe

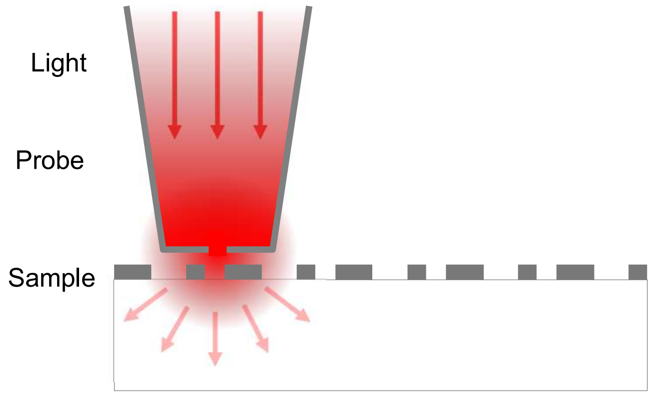

Betzig et al. (1991)

Optical Resolution Beyond the Diffraction Limit

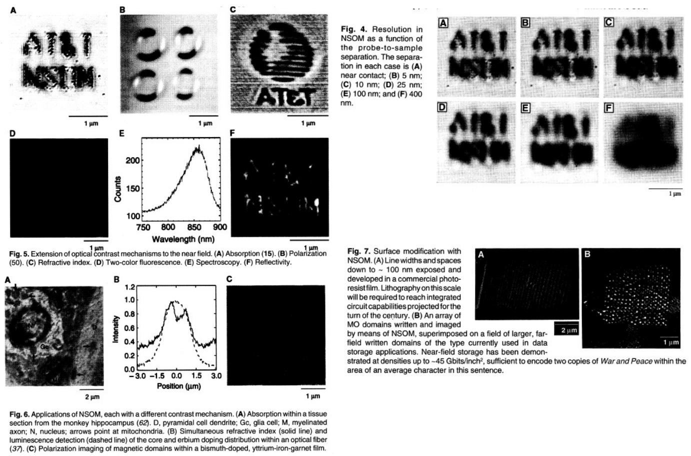

Fig. 4. Resolution in NSOM as a function of the probe-to-sample separation. The separation in each case is (**A**) near contact; (**B**) 5 nm; (**C**) 10 nm; (**D**) 25 nm; (**E**) 100 nm; and (**F**) 400 nm.

Fig. 5. Extension of optical contrast mechanisms to the near field. (**A**) Absorption (**15**). (**B**) Polarization (50). (**C**) Refractive index. (**D**) Two-color fluorescence. (**E**) Spectroscopy. (**F**) Reflectivity.

Fig. 6. Applications of NSOM, each with a different contrast mechanism. (**A**) Absorption within a tissue section from the monkey hippocampus (*62*). D, pyramidal cell dendrite; Gc, glia cell; M, myelinated axon; N, nucleus; arrows point at mitochondria. (B) Simultaneous refractive index (solid line) and luminescence detection (dashed line) of the core and erbium doping distribution within an optical fiber (*37*). (**C**) Polarization imaging of magnetic domains within a bismuth-doped, yttrium-iron-garnet film.

Fig. 7. Surface modification with NSOM. (A) Line widths and spaces down to ~ 100 nm exposed and developed in a commercial photoresist film. Lithography on this scale will be required to reach integrated circuit capabilities projected for the turn of the century. (**B**) An array of MO domains written and imaged by means of NSOM, superimposed on a field of larger, far-field written domains of the type currently used in data storage applications. Near-field storage has been demonstrated at densities up to ~45 Gbits/inch², sufficient to encode two copies of *War and Peace* within the area of an average character in this sentence.

Betzig & Trautman, Science 257, 189 (1992)

Model: Aperture in an infinitely thin ideal conductor

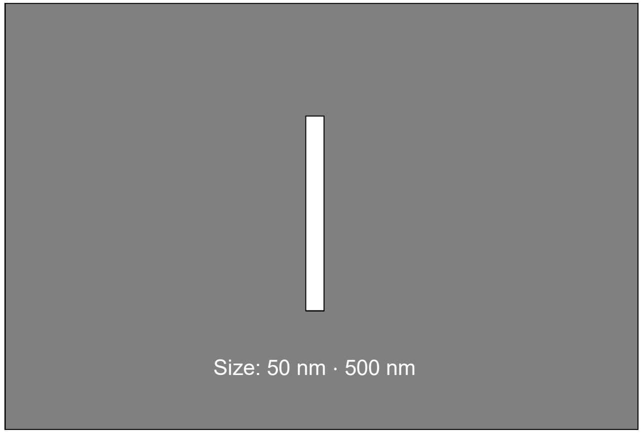

Reflexion at a Metallic Surface

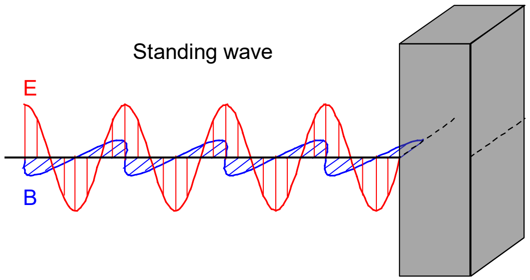

A slit in a metal screen as scatterer for the electromagnetic field

$\vec{E}$ perpendicular to long side of the slit

In first order the fields inside the slit are equal to the fields at the metal surface

- At the edges the tangential components of E and H must be continuous.
- The incoming E-field is cancelled by the opposite field created by the charges at the slit's rim.
- The additional H-field is created by the displacement current $\dot{\vec{D}}$.

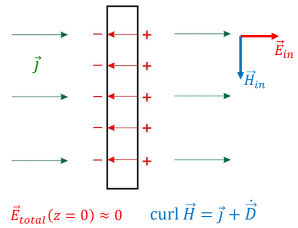

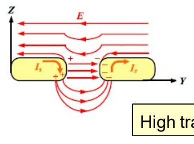

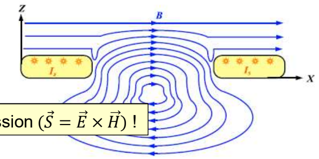

Zakharian et al. (2004)

A slit in a metal screen as scatterer for the electromagnetic field

$\vec{E}$ parallel to long side of the slit

In first order the fields inside the slit are equal to the fields at the metal surface

- At the edges the tangential component of E and the normal component of B must be continuous.
- The incoming E-field is cancelled (at the edges) by induction caused by the magnetic field penetrating the slit.

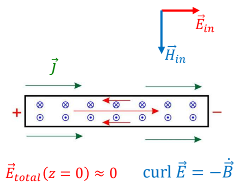

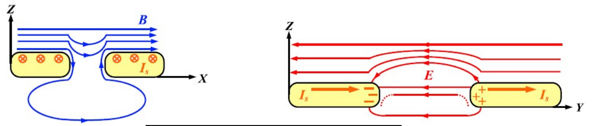

Low transmission ($\vec{S} = \vec{E} \times \vec{H}$) !

Zakharian et al. (2004)

Optical Near-Fields at a Circular Aperture

Hans Bethe
(1906 – 2005)

Christoffel Jacob Bouwkamp
(1915 – 2003)

Wikipedia

Diffraction at a Circular Aperture: Babinet Principle

Circular Disc

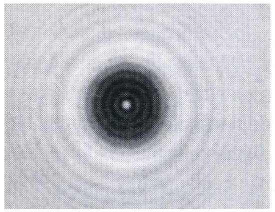

Circular Aperture

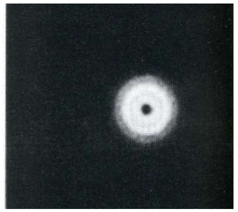

The diffraction pattern at an aperture and a complementary disc are equal in intensity if the undiffracted light is subtracted.

Demtröder, Experimentalphysik 2

Generalized Babinet Principle

for an infinitely thin, ideally conducting film

The following relations hold for the diffracted fields (near- and far-fields) of an aperture A and its complementary disc K:

$$E_A \to -H_K$$
$$H_A \to E_K$$

Near-fields at a circular nano-aperture: approximate solution of Bouwkamp

Oblate-spheroidal coordinates (with radius a of the aperture):

$$z = auv, \quad x = a\sqrt{(1-u^2)(1+v^2)}\cos\varphi, \quad y = a\sqrt{(1-u^2)(1+v^2)}\sin\varphi,$$

where $0 \le u \le 1$, $-\infty \le v \le \infty$, $0 \le \varphi \le 2\pi$. The surfaces $v = 0$ and $u = 0$ correspond to the aperture and the screen, respectively.

Defining equation (spheroid)

$$\frac{x^2+y^2}{1+v^2} + \frac{z^2}{v^2} = a^2$$

Solution for $a \ll \lambda$ (valid for distances to the aperture $r \ll a$):

$$E_x/E_0 = \mathrm{i}kz - \frac{2}{\pi}\mathrm{i}kau\left[1 + v\arctan v + \frac{1}{3}\frac{1}{u^2+v^2} + \frac{x^2-y^2}{3a^2(u^2+v^2)(1+v^2)^2}\right]$$

$$E_y/E_0 = -\frac{4\mathrm{i}kxyu}{3\pi a(u^2+v^2)(1+v^2)^2},$$

$$E_z/E_0 = -\frac{4\mathrm{i}kxv}{3\pi(u^2+v^2)(1+v^2)},$$

$$H_x/H_0 = -\frac{4xyv}{\pi a^2(u^2+v^2)(1+v^2)^2},$$

$$H_y/H_0 = 1 - \frac{2}{\pi}\left[\arctan v + \frac{v}{u^2+v^2} + \frac{v(x^2-y^2)}{\pi a^2(u^2+v^2)(1+v^2)^2}\right]$$

$$H_z/H_0 = -\frac{4ayu}{\pi a^2(u^2+v^2)(1+v^2)},$$

Novotny & Hecht, Nanooptics, p. 190-191

Oblate-spheroidal coordinates

Coordinate transformation:

$$x = a\cosh\mu\,\cos\nu\,\cos\phi \qquad v = \sinh\mu$$
$$y = a\cosh\mu\,\cos\nu\,\sin\phi \qquad u = \sin\nu$$
$$z = a\sinh\mu\,\sin\nu$$

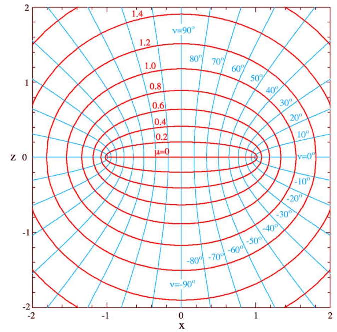

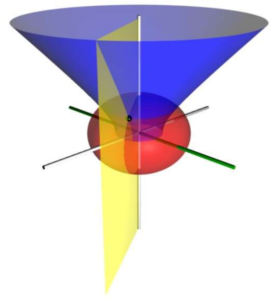

Wikipedia

Transmission through Circular Apertures

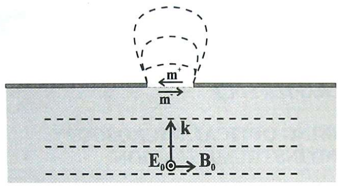

Near-field Intensity along the symmetry axis

$$I(0,0,z) \propto \left(\frac{4kD}{3\pi}\right)^2 \exp\left(-\frac{3\pi z}{2D}\right)$$ with aperture diameter D

Cross section for radiation to the far-field

$$\sigma = \frac{64}{27\pi}k^4 D^6$$

Bouwkamp (1950); M.H.P.Moers (1995)

On-axis intensity behind a circular aperture in an ideal conductor

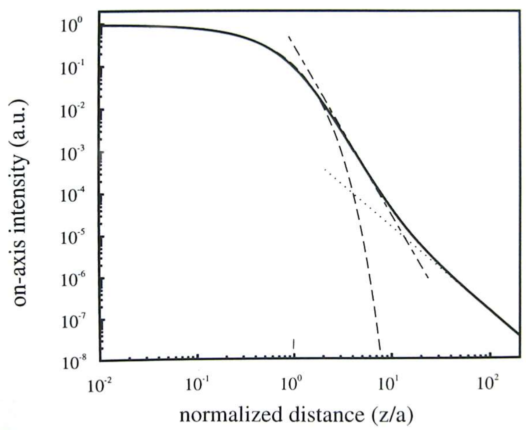

M.H.P.Moers (1995)

Field-Map at an Aperture

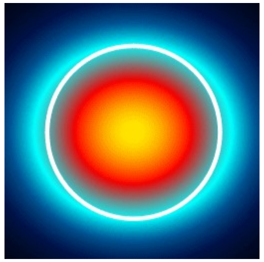

diameter D=50 nm distance 50 nm

Bouwkamp (1950)

Field-Map at a Circular Aperture

d/D = 0.01 0.03 0.05

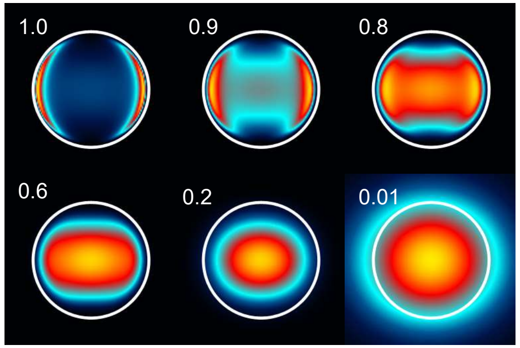

0.1 0.3 1.0